

MODELLING OF THERMAL LOADS OF THE SURGE LINE OF A PWR

M.H.C. Hannink¹, H.J. Uitslag-Doolaard²

¹ NRG, Petten, The Netherlands (hannink@nrg.eu)

² NRG, Petten, The Netherlands

INTRODUCTION

Fatigue is an important ageing mechanism in nuclear power plants. Varying thermal loads are a determining factor in the fatigue life of nuclear components. In design analyses, thermal load fluctuations are often represented by overly conservative assumptions. In the case of long-term operation, it can, therefore, be a challenge to meet the required assessment criteria. Measurement data can help to reduce excessive conservatism. However, signals from a monitoring system are often complex in nature and only known at the distinct measurement locations. In this paper, a method is presented to simulate thermal loads in the surge line of a pressurised water reactor (PWR) in a computationally efficient, simplified way, using measurement data from a plant process monitoring system and a fatigue monitoring system. The temperatures in the structure of the surge line are determined by means of a thermal finite element (FE) analysis. Subsequently, a mechanical FE analysis performed to determine the stresses in the pipes and the nozzles at the pressurizer and main coolant line. The results of the simplified model are validated against simulations with thermal loads from a detailed computational fluid dynamics (CFD) analysis. A comparison is made both in terms of stresses and in terms of fatigue usage.

First, the configuration is described. Then, thermal load modelling by CFD and FE is described, respectively. This is followed by a presentation of the mechanical analyses and fatigue analyses. Finally, the conclusion and discussion are presented.

CONFIGURATION

The study is conducted on the surge line of a typical PWR. The geometry of the configuration is shown in Figure 1. The analyses include the pipes, as well as the nozzles at the pressurizer and main coolant line. The pipes have an inner diameter of 315 mm and consist of 20 mm thick low-alloy steel with a 5 mm thick austenitic stainless steel cladding. The cladding and thermal sleeves are explicitly included in the models.

The results of the thermal analyses are validated with measurement data of a fatigue monitoring system (FAMOS). Three measurement sections (MS) are located at the surge line: one near the pressurizer nozzle, one on the inclined part of the surge line, and one near the main coolant line nozzle (see Figure 2). Each measurement section contains seven thermocouples attached to the outer wall of the pipe (see Figure 2).

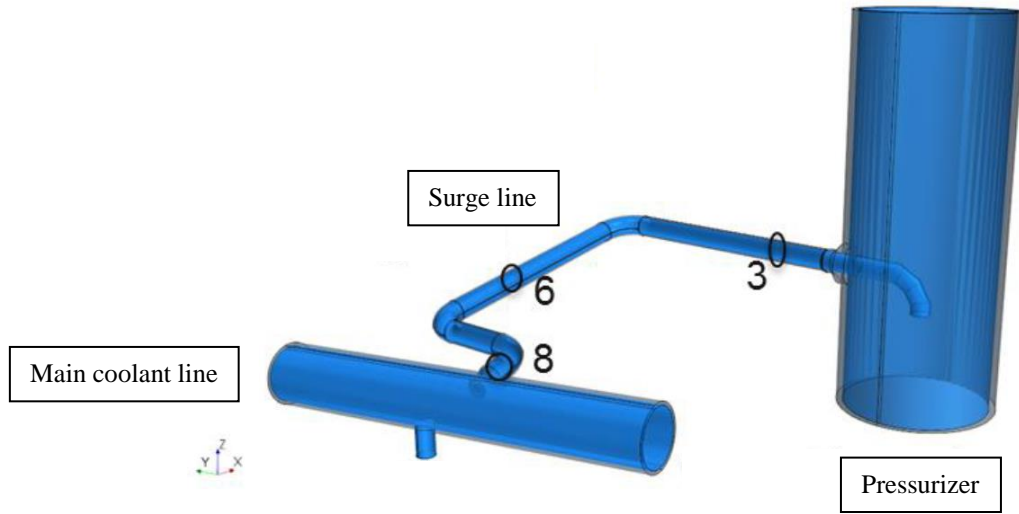


Figure 1. Surge line configuration - computational domain for CFD analysis.

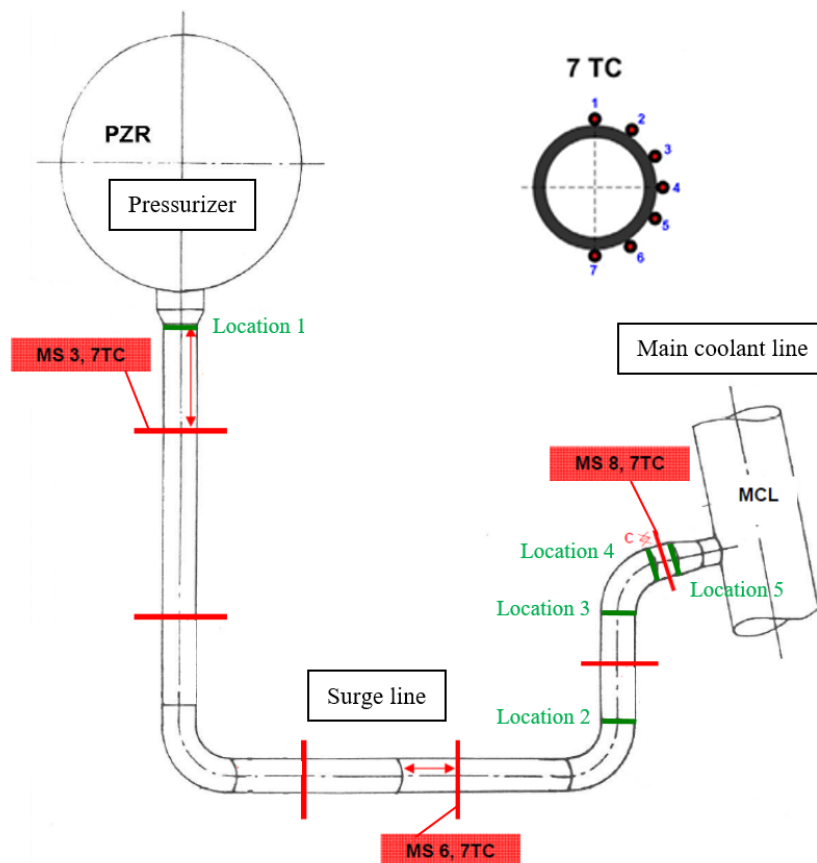


Figure 2. Locations of measurement sections (MS) for fatigue monitoring (red), stress evaluation locations (green), and thermocouple distribution (top right).

THERMAL LOAD MODELLING BY CFD

CFD Model

The thermal loads resulting from the simplified FE method (see next section) are compared to thermal loads generated by a detailed CFD analysis. The CFD analysis, including conjugate heat transfer, is extensively described by Uitslag-Doolaard et al. (2019). The analysis was performed using the commercial software STAR-CCM+, version 11.06. Figure 1 shows the parts of the system incorporated in the model.

The mesh of the surge line and the nozzles at the pressurizer and main coolant line consists of 2.6 million cells in the fluid and 0.5 million cells in the structure (Figure 3). The study by Uitslag-Doolaard et al. (2019) demonstrates that a wall-resolved mesh (using a non-dimensional distance to the wall (y^+) < 1) is required for properly resolving the heat transfer under the transient load.

The top of the pressurizer was taken as a mass flow inlet and the nozzle of the main coolant line was set as a pressure outlet. Inlet and outlet temperatures are based on measurements by the plant process monitoring system. As an initial condition, these temperatures were interpolated over the height of the surge line. The mass flow rate was determined by the change in water level in the pressurizer, which is measured by the process monitoring system as well. Adiabatic boundary conditions were applied at the outsides of the entire structure. The internal pressure of the system was 5.1 bar.

In the study by Uitslag-Doolaard et al. (2019), two turbulence models were tested. Comparison of these models shows that stratification is most accurately predicted with the realizable k - ϵ two-layer model. The analysis presented in this paper spans a period of 3200 seconds, during which two insurge events and one outsurge event occur. A fixed time step of 0.5 seconds with an implicit solver has been demonstrated to yield accurate results. The temporal segregated momentum and segregated energy solvers apply second order schemes.

For the structure, constant material properties were used. The piping and cladding were modelled with a density of 7930 kg/m³ and a specific heat at constant pressure of 490 J/kg·K. Thermal conductivities of 44 W/m·K for the piping and of 16 W/m·K for the cladding were used. For the water, isobaric temperature-dependent properties at 5.1 bar were taken from Lemmon et al. (2018).

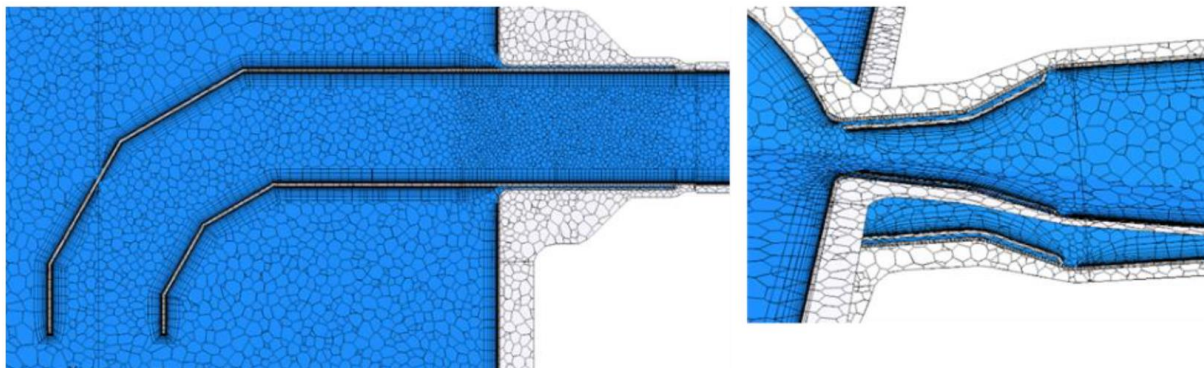


Figure 3. CFD meshes of the pressurizer nozzle (left) and the main coolant line nozzle (right).

CFD Results

The results of the CFD analysis have been validated with measurement data of the fatigue monitoring system. In Figure 4 to Figure 6, the measurements (black lines) of thermocouples 1, 4 and 7 (see Figure 2) are compared with the temperatures resulting from the CFD analysis at the same locations (red lines). The comparison is shown for measurement sections MS 3, MS 6 and MS 8 (see Figure 2). There is a reasonably good agreement between the measurements and analysis results.

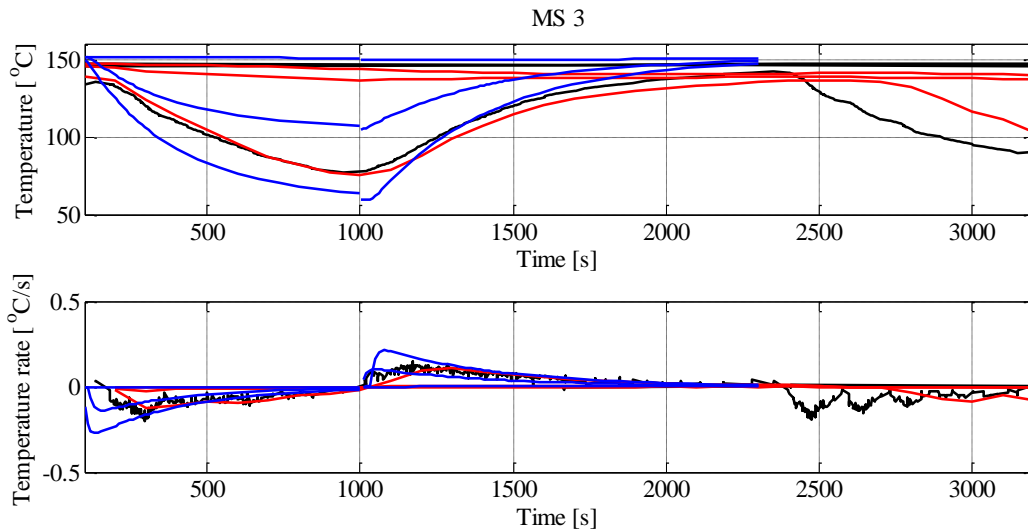


Figure 4. Measured (black) and calculated temperatures (red = CFD analysis, blue = FE analysis).

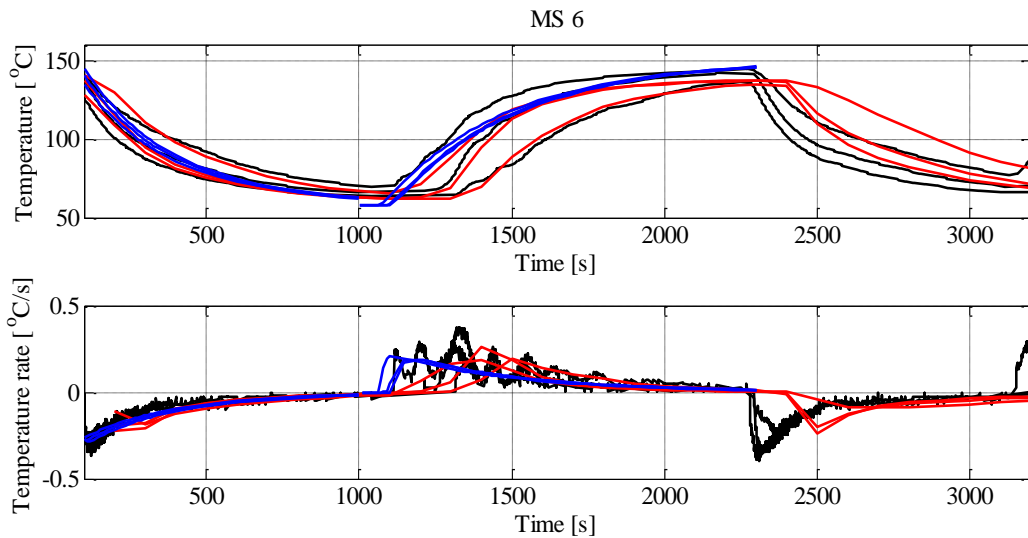


Figure 5. Measured (black) and calculated temperatures (red = CFD analysis, blue = FE analysis).

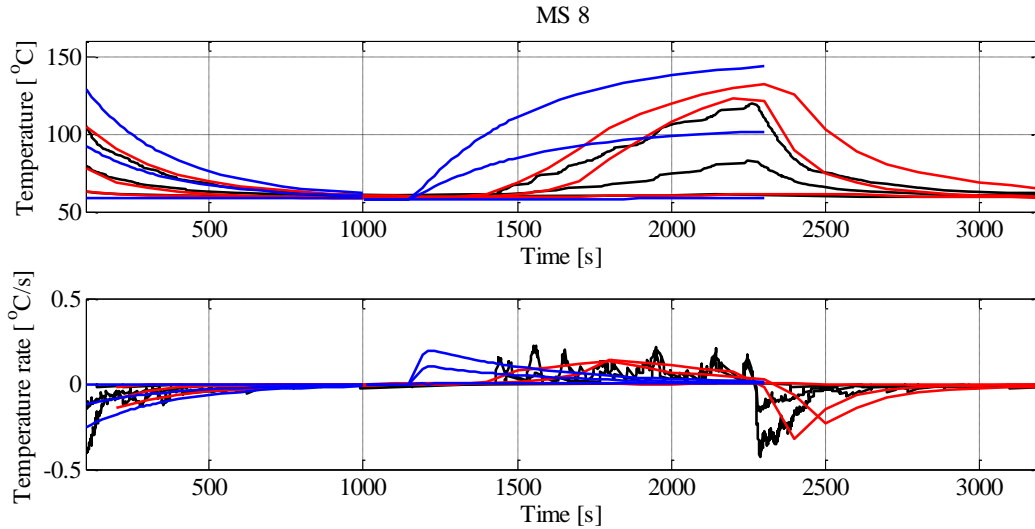


Figure 6. Measured (black) and calculated temperatures (red = CFD analysis, blue = FE analysis).

THERMAL LOAD MODELLING BY FE METHOD

FE Model

In the simplified method, the thermal loads of the surge line are simulated using a thermal FE model of the structure. The surge line and parts of the pressurizer and main coolant line were meshed with eight-node thermal solid elements (Figure 7). The analysis was performed using the FE software ANSYS, version 18.2.

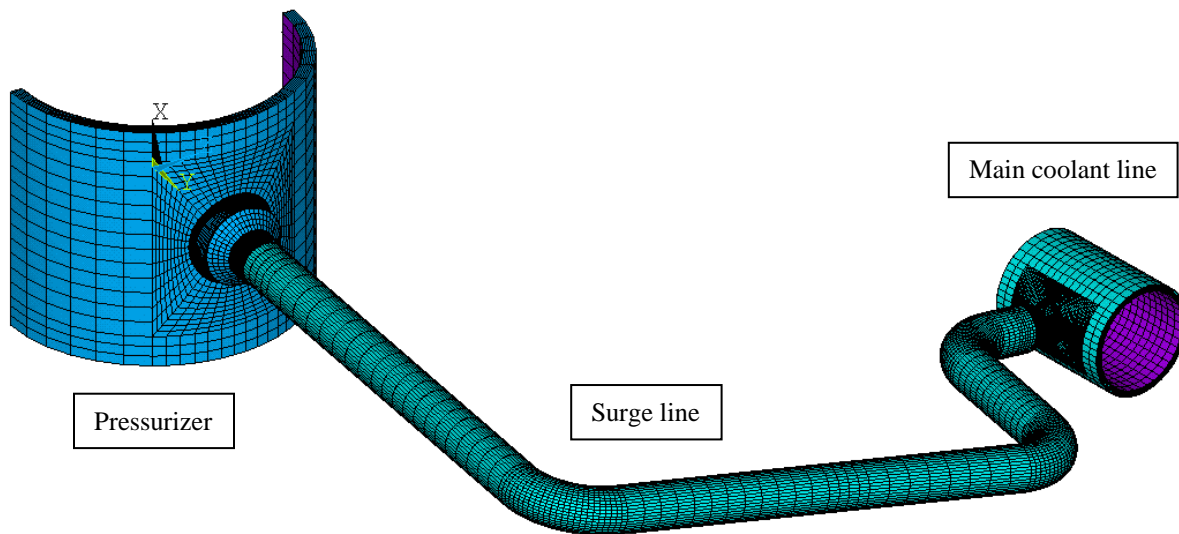


Figure 7. FE model of the surge line.

The temperature fluctuations in the surge line are simulated by applying a convection boundary condition to the inner wall of the pipe. The convection boundary condition is defined by a time-dependent bulk temperature and a constant heat transfer coefficient. Like in the CFD analysis, the exterior boundaries of the system are assumed to be fully insulated (adiabatic).

The bulk temperature is simulated in a simplified way (Figure 8 and Figure 9). Some water in the surge line is assumed to have the same temperature as the water in the pressurizer (red) and the remaining water in the surge line is assumed to have the temperature of the main coolant (blue). The temperatures are based on measurements by the plant process monitoring system. During the simulated period, the maximum pressurizer temperature (red) is 151 °C, and the minimum main coolant temperature (blue) is 58 °C. The interface between the two flows is modelled as a step change in temperature (i.e., no mixing is taking place). During the insurge and outsurge events, the interface between the hot and colder water moves along the surge line, with lowest and highest positions of the interface shown in Figure 8 and Figure 9 respectively.

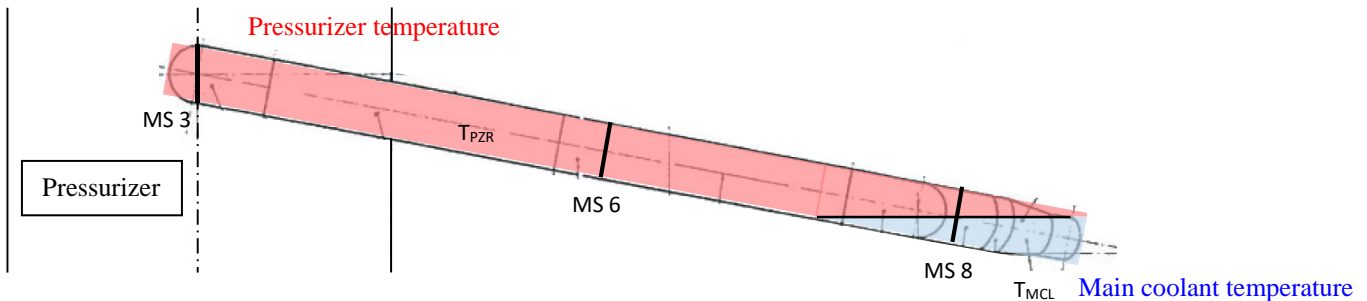


Figure 8. Side view of the initial condition of the insurge event ($t = 0$ s) and the end condition of the outsurge event ($t = 2300$ s).

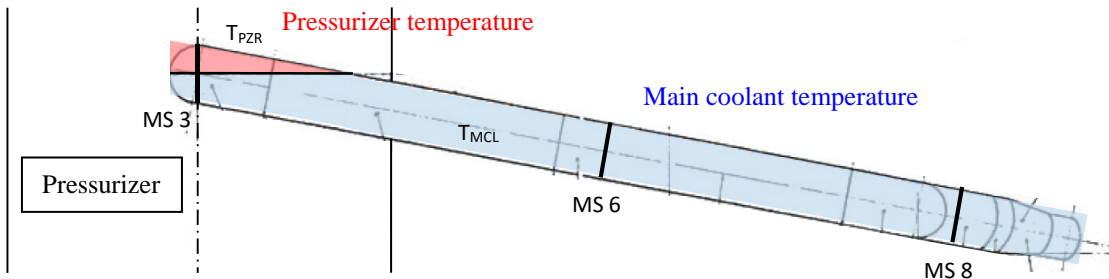


Figure 9. Side view of the end condition of the insurge event and the initial condition of the outsurge event (both at $t = 1000$ s).

At the beginning of the insurge event ($t = 0$), stratification is measured near the main coolant line nozzle (MS 8, Figure 6). At the other two measurement locations, the temperature distribution across the cross-section of the pipe is largely uniform and approaches the pressurizer temperature (MS 3 and MS 6, Figure 4 and Figure 5). To simulate the initial condition of the insurge event, the interface between the hot and colder water is therefore assumed to be at the centre of MS 8 (Figure 8). At the end of the insurge event ($t=1000$ s), the stratification is measured near the pressurizer (MS 3, Figure 4). At the other two measurement locations, the temperature distribution across the cross-section of the pipe is largely uniform and approaches the pressurizer temperature (MS 6 and MS 8, Figure 5 and Figure 6). To simulate the end condition of the insurge event, the interface between the hot and colder water is, therefore, assumed to be at the centre of the horizontal pipe (Figure 9).

During time evolution, the interface moves in vertical direction from the initial position to the final position with a constant velocity. The insurge and outsurge events are simulated in two separate runs, with the initial and final conditions considered as steady-state cases. The insurge event runs from 0 s to 1000 s and the outsurge event from 1000 s to 2150 s. To make a meaningful comparison, the same structural material properties are used as in the CFD analysis. The heat transfer coefficient was determined by an empirical relation for a fully developed turbulent flow in cylindrical pipe (Incropera and DeWitt, 1990), where the flow velocity was derived from the level measurements in the pressurizer. Conservatively, the

maximum values of the flow velocities and water properties at maximum temperature were used. This approach yields a heat transfer coefficient of 421 W/m²K for the insurge event and a heat transfer coefficient of 292 W/m²K for the outsurge event.

FE Results

Figure 4 to Figure 6 show the temperatures resulting from the FE analyses (blue lines). During insurge and outsurge, the interface between the hot and colder water moves along the surge line. At the locations where the interface passes, the inner wall of the pipe will experience a step change in temperature (i.e., a very large temperature rate of change). Due to thermal inertia, the response of the outer wall of the pipe will lag behind, so the maximum temperature rate measured at the outer wall (Figure 4 to Figure 6) is much lower than the temperature rate at the inner wall.

Figure 4 to Figure 6 also show the comparison of the calculated temperatures (blue lines) with the measurements from the fatigue monitoring system (black lines). The calculated stratification profiles represent the general trends of the measurement signals, but do not show an exact match. This is mainly due to the simplifications that were made in the FE model. In the FE model, steady-state initial and final conditions have been assumed. In reality, the hot and colder water is continuously moving back and forth through the surge line, so no steady state is reached. Furthermore, the real flow is not moving exactly from or up to the centres of the measurement sections, like assumed in the FE model (see Figure 8 and Figure 9). See for example MS 3 in Figure 4, at $t = 1000$ s, where only the temperature of the bottom thermocouple has changed (lower black line). A third simplification influencing the calculated stratification profiles is the fact that no mixing is modelled between the hot and colder water. A fourth simplification is that in the FE model, the water flows with a constant velocity through the pipe whereas in reality the fluid velocity fluctuates. In the next section, the impact of these simplifications on the calculated stresses is demonstrated.

MECHANICAL ANALYSES

Model

To calculate the stresses in the surge line, mechanical FE analyses were performed. In all cases, the same mesh was used as for the thermal FE analyses (Figure 7), where the thermal elements were changed into eight-node structural solid elements. The austenitic steel cladding and the low-alloy main material were modelled using temperature-dependent material properties.

In the mechanical analyses, only thermal loads were applied. In the first analysis, the temperature distribution in the structure, resulting from the CFD analysis, was mapped onto the FE mesh (see Figure 10 and Figure 11, left). This mechanical analysis was performed for a period of 3200 seconds, with a fixed time step of 100 seconds. In addition, other FE analyses were performed with thermal loading taken as the temperature distributions in the structure resulting from the thermal FE analyses (see Figure 10 and Figure 11, right). Like the thermal FE analyses, two separate analyses were performed for the insurge event running from 0 s to 1000 s, and the outsurge event from 1000 s to 2150 s, respectively.

At the longitudinal edges of the pressurizer, symmetry conditions were applied by suppressing the degrees of freedom in global y-direction (Figure 7). This allows the vessel to expand freely in the radial direction. Expansion in axial direction takes place with respect to the support lug at the bottom of the pressurizer, which was simulated by prescribing a temperature-dependent axial displacement Δx (Figure 7) at the bottom edge of the modelled section. Thermal expansion of the main coolant loop was taken into account by prescribing temperature-dependent displacements and rotations at one end of the modelled section of the main coolant line. The displacements and rotations result from a pipe stress analysis. At the opposite end of the main coolant line section, a rigid surface constraint was applied, but no displacements

and rotations were prescribed. A rigid surface constraint was also applied at the bottom of the thermal sleeve of the surge-line nozzle of the pressurizer.

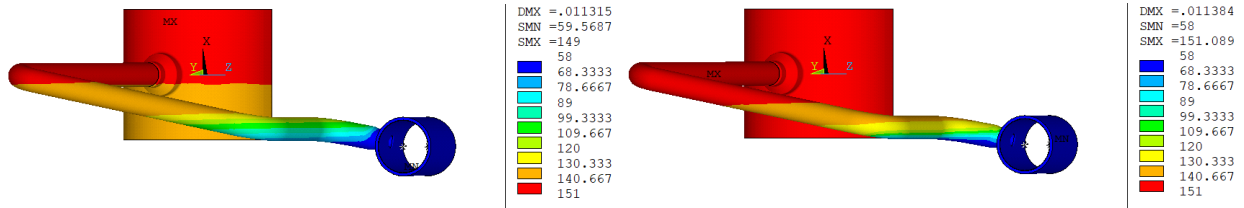


Figure 10. Thermal loading [°C] at the start of the insurge event (t = 100 s), result of CFD analysis (left) and result of FE analysis (right).

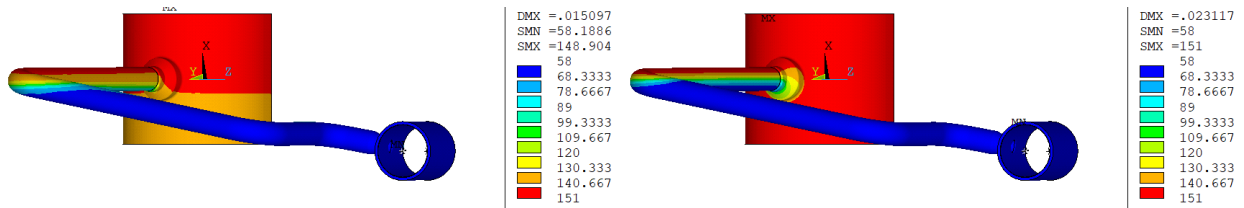


Figure 11. Thermal loading at the start of the outsurge event (t = 1000 s), result of CFD analysis (left) and result of FE analysis (right).

Results

Figure 12 and Figure 13 show the calculated stress intensity distributions at the starts of the insurge and outsurge events. The stress intensities due to thermal loads, resulting from the CFD and FE analyses, show similar trends. The influence of the different modelling techniques on the fatigue usage is presented in the next section.

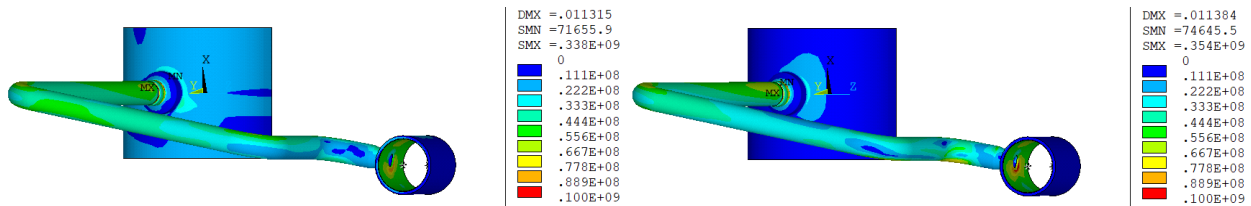


Figure 12. Stress intensity [Pa] at the start of the insurge event (t = 100 s), result of CFD analysis (left) and result of FE analysis (right).

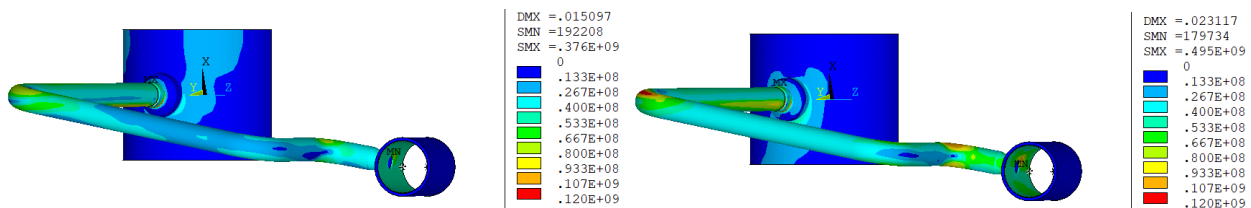


Figure 13. Stress intensity [Pa] at the start of the outsurge event (t = 1000 s), result of CFD analysis (left) and result of FE analysis (right).

FATIGUE ANALYSES

The fatigue assessment is performed according to ASME Boiler and Pressure Vessel Code, Section III, Appendices, XIII-3520 and XIII-3450 (2019), using the design fatigue curves for austenitic steels and low-alloy steels. The design fatigue curves were implemented up to and including 10^7 cycles. Fatigue usage is evaluated at the five locations most relevant for the fatigue behaviour of the piping (see Figure 2, locations 1 to 5). At each location, the results are evaluated at 16 circumferential positions (0° , 22.5° , 45° ... 337.5°), with 0° being at the top of the component, and 180° being at the bottom. When following the nozzles and the surge line from the pressurizer side to the main coolant line side, the angles defining the positions increase clockwise. Results are evaluated both on the inside and outside of the piping. Because locations 1 to 5 are (as-welded) welds, fatigue strength reduction factors of 1.8 were applied in the directions perpendicular to the welds.

Figure 14 shows the fatigue usage per cycle for the five locations. The highest fatigue usage is found in the bottom region of the pipes. Fatigue usage for the thermal loads resulting from the CFD analysis is relatively low and in many cases zero (which means that the alternating stress intensities are smaller than the alternating stress intensities corresponding to 10^7 cycles on the design fatigue curves). Fatigue usage due to thermal loads resulting from the FE analyses is generally slightly higher. Therefore, it can be concluded that the simplified way of modelling thermal loads leads to a conservative representation of the analysed transients.

CONCLUSION AND DISCUSSION

In this paper, a computationally efficient, simplified method for modelling thermal loads on the surge line of a PWR was presented. The results obtained with this method have been validated with results from a detailed CFD analysis and using temperatures recorded by a fatigue monitoring system. After a comparison of the temperatures, the stresses and fatigue usage were also compared. The results show that the simplified way of modelling thermal loads leads to a conservative representation of the analysed transients at the assessed locations. Because the evaluated fatigue loads are relatively small, it is recommended to extend the validation in further research with larger transients and transients travelling through different parts of the surge line. In addition to the welds in the piping, the thermal sleeves of the nozzles at the pressurizer and main coolant line are also known to be fatigue relevant locations. Therefore, detailed evaluation of the influence of the discussed modelling techniques on the fatigue usage of the connections of the thermal sleeves to the nozzles is recommended for further research as well.

REFERENCES

- Incropera, F.P. and DeWitt, D.P., (1990). *Fundamentals of heat and mass transfer*, 3rd ed., John Wiley & Sons.
- Lemmon, E.W., McLinden, M.O. and Friend D.G., "Thermophysical Properties of Fluid Systems" in *NIST Chemistry WebBook*, NIST Standard Reference Database Number 69, Eds. P.J. Linstrom and W.G. Mallard, National Institute of Standards and Technology, Gaithersburg MD, (retrieved 2018).
- Uitslag-Doolaard, H.J., De Bont, C.G.M., Roelofs, F. and Blom, F.J. (2019). "Combined Thermal-mechanical and Thermal-hydraulic Analyses in a Pressurized Surge line," *Proc., ICAPP*, Juan-les-pins, France, Paper 00161.
- ASME Boiler & Pressure Vessel Code, Section III, Appendices* (2019). The American Society of Mechanical Engineers.

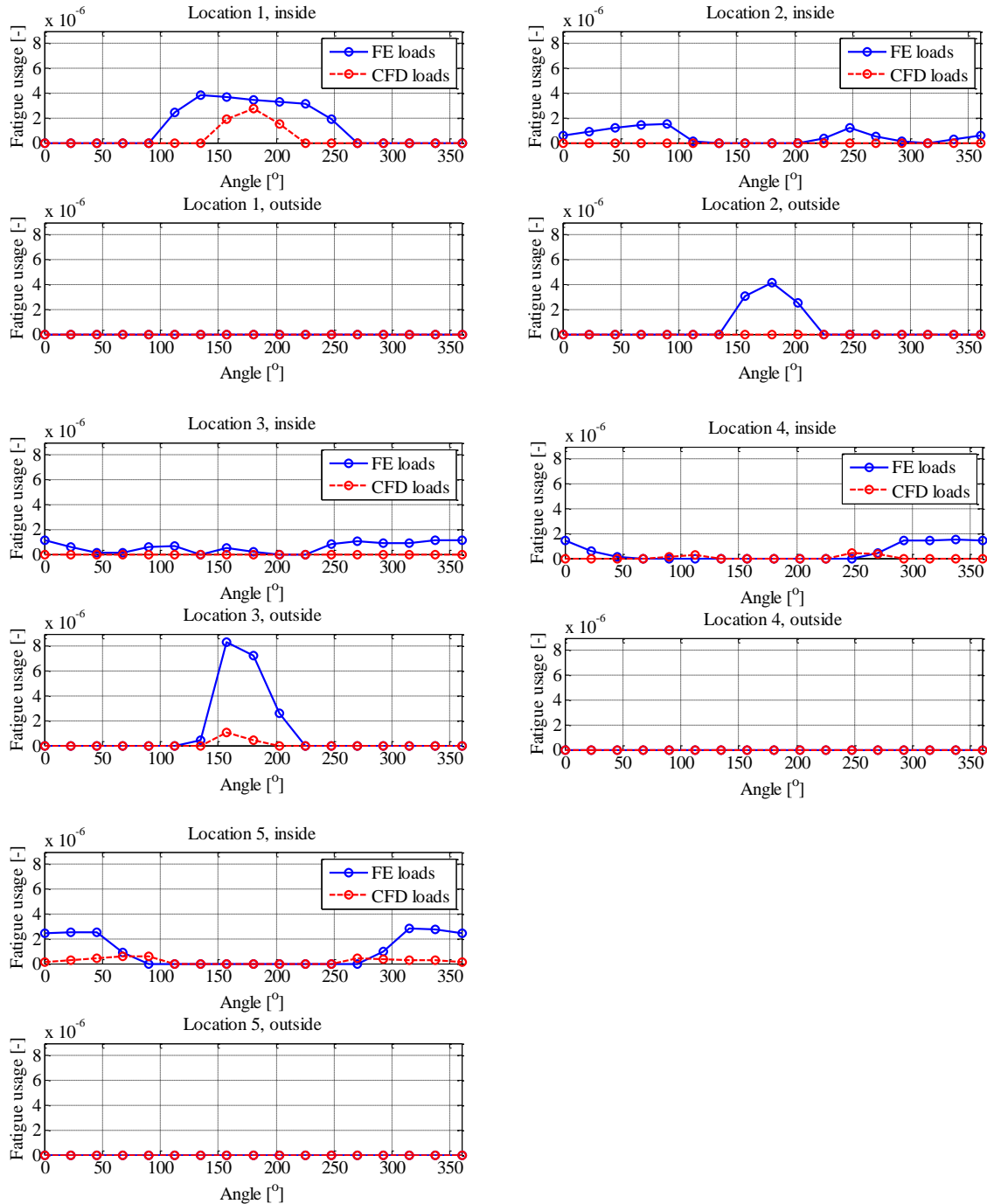


Figure 14. Fatigue usage per location per cycle.

Disclaimer

Goods labelled with an EU DuC (European Dual-use Codification) not equal to ‘N’ are subject to European and national export authorization when exported from the EU and may be subject to national export authorization when exported to another EU country as well. Even without an EU DuC, or with EU DuC ‘N’, authorization may be required due to the final destination and purpose for which the goods are to be used. No rights may be derived from the specified EU DuC or absence of an EU DuC.